

DOI: 10.17951/pjss/2020.53.2.293

PIOTR BARTMIŃSKI*, MARCIN SIŁUCH*

SPATIAL RESAMPLING OF REMOTE SENSING DATA –
ACCURACY VS. REDUNDANCY

Received: 12.05.2020

Accepted: 30.11.2020

Abstract. Active surface reflectance in a UV/VIS/NIR range deserve special attention among remote sensing techniques due to the potential of information it carries. Data are diversified in terms of spatial, spectral and temporal resolution, resulting in differences in data comparison and collection of material that may be redundant. The aim of the study was to assess whether the use of high-resolution data in analysis of an intensively used meadow is justified. 116 images from Planet sensor were analysed, registered from 2016 to 2019. NDVI, EVI and GLI were calculated for all of the terms. Resampling of data was carried out, with the use of 30 m grid, prepared on the basis of 3 m Planet pixel. Data with different resolution was compared. Seasonal course of values was similar in all cases, values of chosen deciles were nearly the same, however, differences in minimum and maximum values were noted. It was concluded that the use of high-resolution data is not advisable in the context of the spatial variability of seasonal vegetation indices in the case of a terrain with homogeneous land cover. Values of structurally simplified indices are less homogeneous than that of indicators consisting of a greater number of modifying factors.

Keywords: active surface reflectance, vegetation index, data resampling

* Department of Geology, Soil Science and Geoinformation, Maria Curie-Skłodowska University in Lublin, Kraśnicka 2cd, 20-718 Lublin; corresponding author: piotr.bartminski@umcs.pl

INTRODUCTION

Remote sensing techniques are an extremely important source of data providing information used in environmental protection (Melesse *et al.* 2007), agriculture (Palanisamy *et al.* 2019), spatial planning, and many other fields of science (Heiskanen *et al.* 2017).

Due to their potential, data on active surface reflectance in a wide spectrum range from UV through VIS to NIR deserve special attention among many types of data. They are especially valuable for analyses of vegetation cover (Teillet *et al.* 1997, Purevdorj *et al.* 1998).

Analyses of the properties of vegetation most often involve calculation of the ratios of reflected signals at different electromagnetic wavelengths, which is the basis for calculation of the so-called reflectance indices, often called “plant indices” due to their most common application (Huete 1988, Bannari *et al.* 1995, Liu K. *et al.* 2020).

Data are acquired with the use of various sensors differing in their spatial and spectral resolutions (Sharma *et al.* 2020, Kim *et al.* 2020). Obviously, data with the highest spatial resolution have a local character. The use of airplanes or unmanned aerial vehicles facilitates acquisition of data with pixels in the range of several millimetres; however, besides the local scale, this poses a problem with processing large volumes of data. Satellite sensors facilitate simultaneous recording of scenes with a surface area of a few to several dozen square kilometres, but their resolution ranges from a few to several dozen meters (Mancino *et al.* 2020).

The spectral resolution is associated with variable image recording. Images in the visible RGB spectrum captured by inexpensive sensors with wide spectral channels available in various scales and mounted in various platforms are the most common (Barrero and Perdomo 2018, Marín *et al.* 2020). Multispectral imaging techniques, which combine near-infrared radiation data with the basic channels, are becoming increasingly popular (Fawcett *et al.* 2020). Selected sensors record the image of the active surface in more than several tens of channels (hyperspectral imaging) with a varying number of registered channels and total recording range. The most common cameras recording radiation in the 400–1,000 nm range are widely used in many branches of science (Thenkabail *et al.* 2019).

Remote sensing data also vary in terms of temporal resolution – satellite sensors record the same area in specific time sequences usually associated with the position of the sun above the horizon. Data obtained in this way are comparable with each other, as the angle of incidence of sunrays on individual days is similar.

In recent years, research has been undertaken to assess the possibility of comparison of data with different spectral resolutions by means of resampling thereof, which is defined as generation of information from different sources in

the same spatial resolution and uniform geometry. There are also attempts to find a compromise between the spectral resolution, spatial resolution, and data retrieval costs associated with data extraction and acquisition (Caras *et al.* 2017, Prey and Schmidhalter 2019, Lyons *et al.* 2018).

The aim of the present study was to fill the gap in determination of a spatial resolution that is sufficient for vegetation analysis of approx. 40-ha intensively used meadows. The application of appropriate methods will reduce the costs of retrieval of data for various purposes in the future. Limitation of the resolution also facilitates synthesis of data and reduction of errors associated with too high resolution.

The objective of the study was to assess whether the use of high-resolution data in analysis of vegetation in an intensively used meadow with a homogeneous cover is advisable or whether it generates a large amount of redundant information. An additional goal was to compare different methods of data resampling in a multi-season scale.

MATERIALS AND METHODS

The study was carried out in an object located in Andrzejów. It is an intensively used meadow with a homogeneous species composition located in Polesie Lubelskie, approx. 5 km from Urszulin (Fig. 1). Its substrate is a large peat bog subjected to drainage in the last century, which was intended to lower the groundwater table and convert the land into permanent grassland. Currently, the soil cover of the area consists of thick muck soils formed on fens and transitional peat bogs.

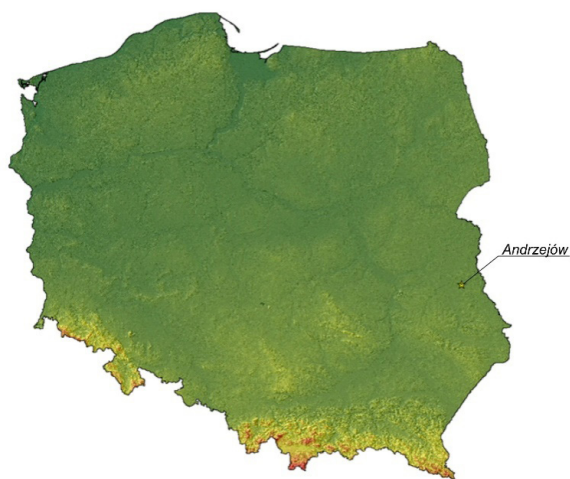


Fig. 1. Location of research area

A set of data provided by the Planet sensor (Planet Team 2020) registered between August 19, 2016 and April 19, 2019 was used for the study. The data were selected based on the assumption of a cloud cover over the analysed object as low as <10% and land cover >90%. Satellite data registered between 9:00 and 10:00 UTC were used.

A grid was prepared for further analysis; the mesh size was based on the imaging pixel (3 m), and the total grid size was 1,050 m × 1,050 m (Fig. 2). To compare data with different resolutions, a 30-m grid was superimposed on the 3-m grid (one pixel contained 100 basic pixels). After verification of the data, 116 images were finally analysed (Table 1).

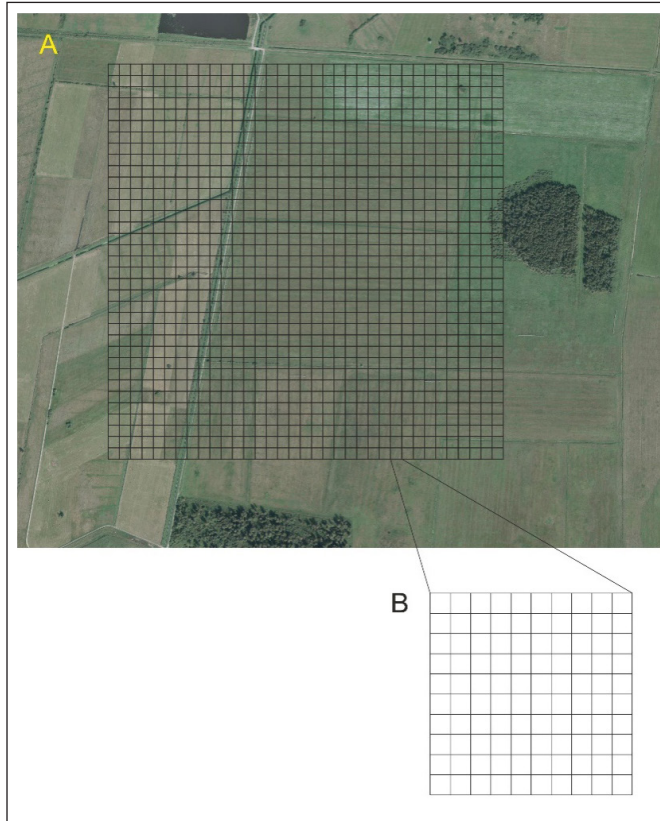


Fig. 2. Scheme of the study; (A) basic grid of 30-m pixels on the background of the orthophotomap, (B) division of 30-m pixel into 100 smaller 3-m pixels

Indicators EVI, GLI, and NDVI were calculated for each of the terms. Average, maximum, and minimum values as well as variability were calculated for each term and each pixel.

Next, data resampling (3-m pixel) was carried out using three methods implemented in the Arc-Gis environment: i) NEAREST – nearest neighbour,

which minimizes changes to pixel values since no new values are created, ii) BILINEAR – calculating the value of each pixel by averaging (weighting for distance) the values of the surrounding four pixels, and iii) CUBIC – calculating the value of each pixel by fitting a smooth curve based on the surrounding 16 pixels (Hall and Meyer 1976, Press *et al.* 1992). Additionally, the values of 100 pixels contained within one large pixel were averaged arithmetically.

Table 1. List of images used in the research

Season	Number of scenes
Summer 2016	4
Autumn 2016	1
Winter 2017	1
Spring 2017	8
Summer 2017	13
Autumn 2017	6
Winter 2018	1
Spring 2018	32
Summer 2018	24
Autumn 2018	14
Winter 2019	1
Spring 2019	9

The data in the original resolution (3 m) were compared with the resampled (30 m) data using the nearest-neighbour method. Differences between the maximum and minimum values were calculated for each of the terms and the two resolutions, and the maximum and minimum values as well as the value of the 1st, 5th, and 9th decile for both spatial resolutions were compiled.

Next, only a part of the scene with the homogeneous meadow was subjected to detailed analysis to check the effect of the surface homogeneity on the results. Nine 30-m pixels characterizing the highly homogenous meadow were chosen. Next, ten 3-m pixels were selected randomly within each of them and statistical analysis (R^2 and Person correlation) of the multi-season values of NDVI, EVI, and GLI was carried out.

RESULTS

The examined area showed spatial diversity of values of particular indicators (Fig. 3).

The differences in the maximum NDVI values recorded for the larger and smaller pixel were relatively small and did not exceed 15% in any of the terms, with an average of 3% (Fig. 4). Substantially greater variability can be observed in the minimum values; in particular, the values recorded in the autumn of 2018

and in the winter of 2019 were drastically different from the others (681 and 257% difference). When these values were excluded, the differences reached up to 63%, with a mean of 13%.

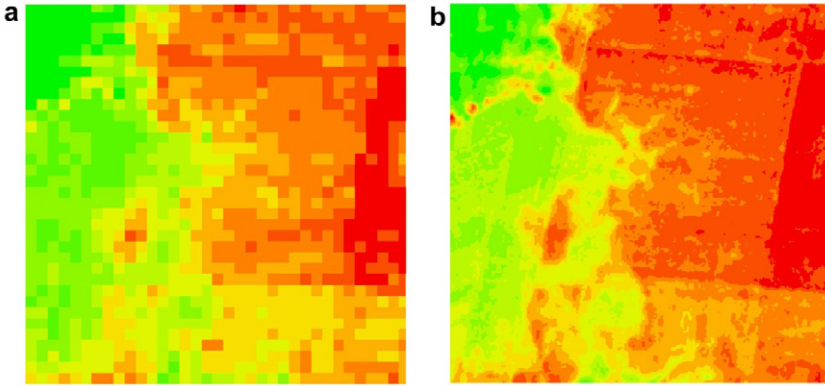


Fig. 3. An example picture of spatial variability of vegetation indices – NDVI, 12.08.2018; (a) 30 m resolution; (b) 3 m resolution

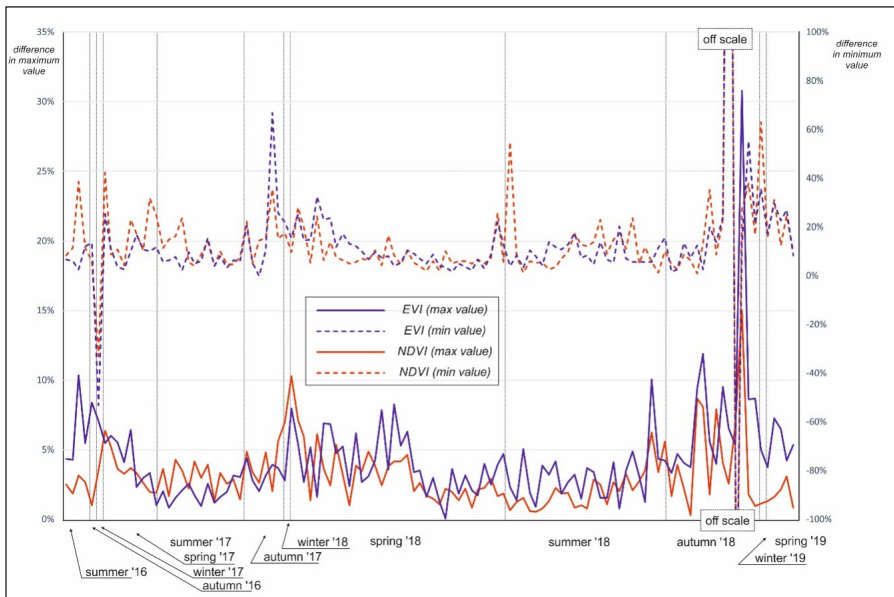


Fig. 4. Percent differences between the maximum and minimum values of EVI and NDVI at different spatial resolutions in a multi-season aspect

The differences in the maximum EVI value exhibited distinct multi-season variability, with significant differences in the early spring of 2019, autumn 2018, spring 2018, and summer 2016. The fluctuations reached up to 31%, with a mean of 4%. In the case of the minimum values, drastic differences were noted

in the same terms as in the case of NDVI (-158% to 712%). After exclusion of the extreme values, the differences reached 67%, with a mean of 11%.

The largest discrepancy between the values of the large and small pixels was exhibited by GLI (Fig. 5). In the case of the maximum values, the difference was on average 19% with a maximum value of nearly 300% (winter 2017). In the case of the minimum values, there were differences in another range: with an average value of 60% and a maximum of 885 and -766%. In turn, the values in two other terms (spring and autumn 2018) differed by two orders of magnitude.

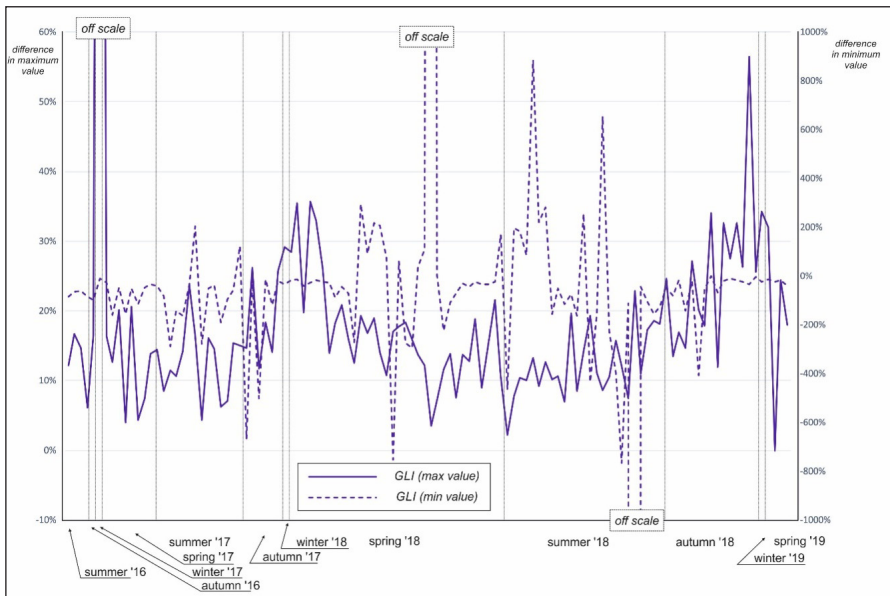


Fig. 5. Percent differences between the maximum and minimum values of GLI at different spatial resolutions in a multi-season aspect

It was assumed that the large discrepancy between the maximum and minimum values resulted from single measurements in single small pixels corresponding to small terrain fragments that differed considerably from the others (roads, ditches, etc.). In order to eliminate the effect of the extreme values on the observations, the course of the 1st, 5th, and 9th decile values in the multi-season scale was determined at both spatial resolutions. The values of the selected deciles demonstrated a surprisingly similar course of all indices, with a correlation exceeding 0.99. The variability level is well illustrated by the combination of absolute maximum and minimum values and selected percentiles (Fig. 6–8).

The multi-season course of NDVI, EVI, and GLI for the randomly selected 3-m and 30-m pixels in the homogeneously used meadow varies. The highest similarity of values can be observed at both resolutions in the case of EVI: the

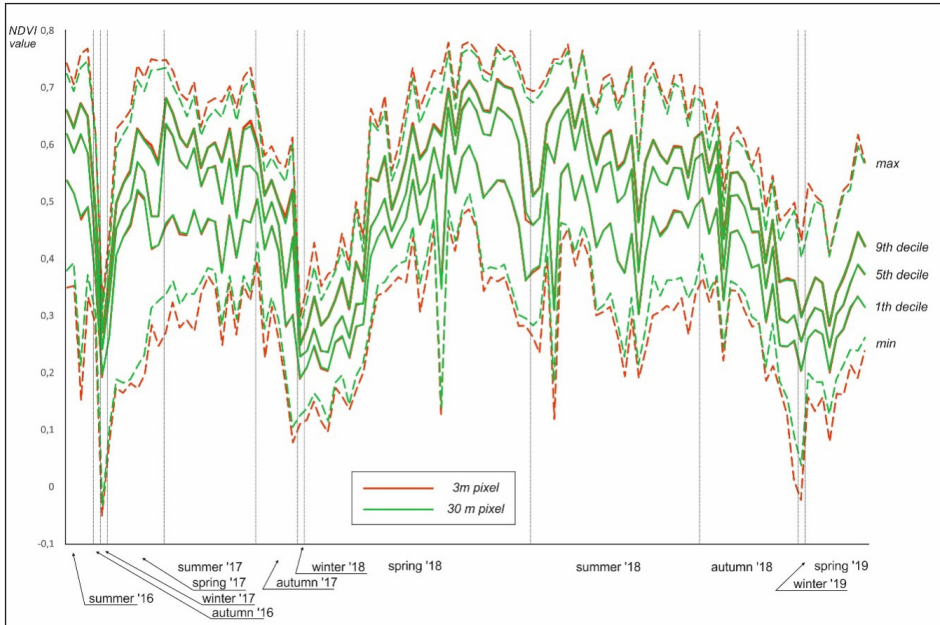


Fig. 6. Multi-season course of the maximum and minimum values as well as the 1st, 5th, and 9th deciles of NDVI in the analysed area for two spatial resolutions. The decile values are overlapping

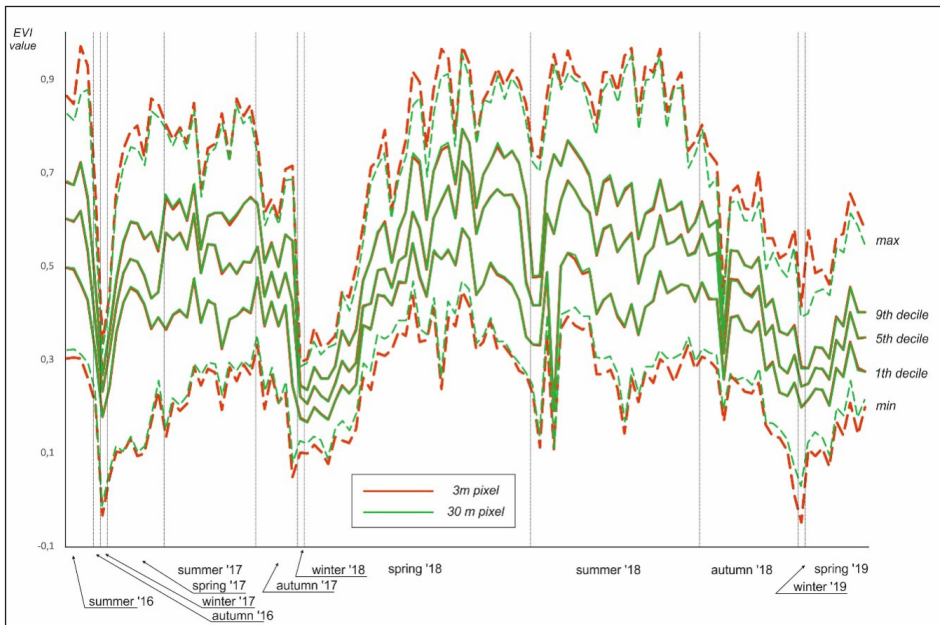


Fig. 7. Multi-season course of the maximum and minimum values as well as the 1st, 5th, and 9th deciles of EVI in the analysed area for two spatial resolutions. The decile values are overlapping

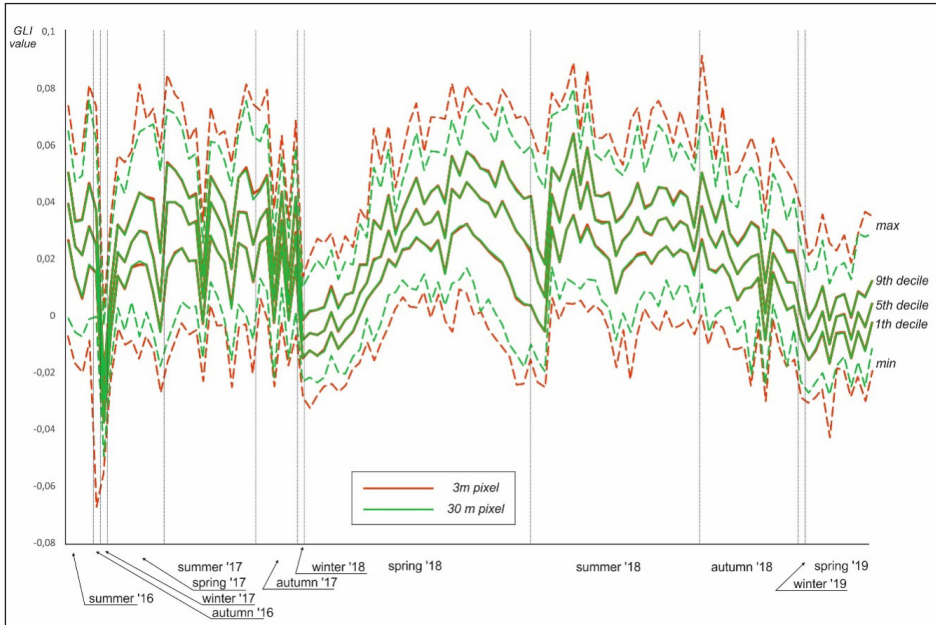


Fig. 8. Multi-season course of the maximum and minimum values as well as the 1st, 5th, and 9th deciles of GLI in the analysed area for two spatial resolutions. The decile values are overlapping

correlation was estimated at 0.95–0.99 and the R^2 coefficient was in the range of 0.65–0.99 (Fig. 9). A substantially lower correlation was found for NDVI (correlation 0.79–0.96, R^2 0.62–0.92) and GLI (correlation 0.75–0.95, R^2 0.55–0.9). The variation of the values was not observed in the case of the small pixels, and the average values were significantly lower than those of EVI.

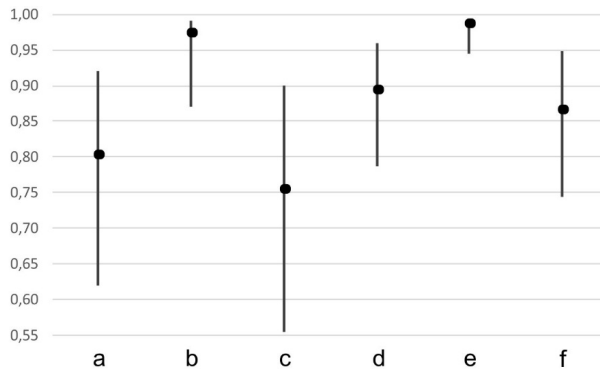


Fig. 9. The results of comparing the course of the studied indicators in 3-m and 30-m pixels; the graph shows the maximum, minimum and average values for 90 3-m pixels compared with the corresponding 30-m pixels; (a–c) R^2 coefficient for NDVI, EVI and GLI, respectively; (d–f) Pearson correlations for NDVI, EVI and GLI, respectively

Additionally, we attempted to determine the impact of the resampling method on the spatial diversity of the analysed indices. The correlation between the values of the indices resampled with the different methods (Table 2) indicates that the three basic methods for spatial data resampling were fully consistent in the analysed case. This was especially evident in the case of the bilinear and cubic methods, although the results of the most common nearest-neighbour method did not differ from the others either. In contrast, the results interpolated with the use of the arithmetic mean of the resampled pixels in the case of NDVI and GLI differed substantially. A high similarity of values was noted in the case of EVI as well.

Table 2. Pearson correlations between 30-m matrices calculated with the use of various methods

Resampling method	NDVI	EVI	GLI
Nearest neighbour – bilinear	0.99881	0.99859	0.99259
Nearest neighbour – cubic	0.99876	0.99854	0.99229
Nearest neighbour – average	0.79040	0.98465	0.77347
Bilinear – cubic	0.99996	0.99996	0.99972
Bilinear – average	0.79090	0.98803	0.77894
Cubic – average	0.79023	0.98728	0.77558

DISCUSSION

The analysed vegetation indices have been extensively investigated for many years. Recently, new indices have appeared or those applied previously have been modified (Fraga *et al.* 2014, Moreira *et al.* 2017, Karkauskaite *et al.* 2017, Tao *et al.* 2020). The choice of an indicator that best reflects the characteristics of vegetation in a given area is always a problem. There is a need for a compromise between the product quality and the logistic and technological possibilities (Xue and Su 2017).

The course of the values for all the analysed indices was similar (Sousa *et al.* 2019). The lowest differences in their values were observed in the autumn and winter periods. During the spring increase in plant photosynthetic activity, the spatial distribution of the indices started to vary significantly and exhibited the greatest variability in the value before the first mowing (at the beginning of summer). The other decline in the values of all indices recorded at the beginning of autumn was caused by another mowing round.

The variability of NDVI, which is based on the RED and NIR channels, was much lower than that exhibited by GLI; nevertheless, the effect of information derived only from the observations of vegetation was very strong. This was similar in the case of EVI, where the course was equally strongly correlated with seasonality but was burdened with a smaller error derived from the atmosphere and background (Huete *et al.* 2002).

The design of the EVI indicator seems to be optimal for the characteristics of meadow communities, as it includes the gain factor, i.e. enhancement of the vegetation signal, and simultaneously the atmospheric resistance RED and BLUE coefficients as well as the canopy background correction factor. The NDVI and EVI values were highly similar throughout the study period, which is largely related to the use of a similar configuration of the channels for spectral information.

The dissimilarity of GLI from the other indicators is associated with the strong influence of green on the values, which is of great importance in the case of mixed pixels and pixels that not directly related to vegetation: the values for the small 3-m pixels were drastically different from the resampled value for the large pixel. Nevertheless, the course of GLI was consistent with the course of the other indices, which may support its suitability when only an RGB camera is available.

In recent years, numerous studies have been conducted to fuse data from sensors with different spatial and spectral resolutions, including fusion of data from multi- and hyperspectral sensors (Hwang *et al.* 2011, Liu W. *et al.* 2020, Ovakoglou *et al.* 2020). Some investigations have confirmed the possibility of using low-resolution data to infer point values or to refer to a substantially higher field resolution, with high correlations between data sequences with a differing spatial dimension (Shirsath *et al.* 2020). It is significant that the literature provides information about the possibility of using low-resolution data in the upscaling process in the case of EVI (Ovakoglou *et al.* 2020), whose resampling potential has also been confirmed in this study. Gao *et al.* (2020) effectively fused data from Landsat and MODIS sensors and obtained a high correlation of selected NDVI values; the correlation was clearly higher for grasslands than for lands managed in another way. Similar results were obtained by Li *et al.* (2014) based on analogous data from the same sensors. In turn, Caras *et al.* (2017) analysed coral reefs using data from various high-resolution sensors. The authors concluded that substrate mixing plays a major role in noise creation and a decrease in accuracy. This inference is correct in the case of a research object with a complex structure, but is not confirmed in the case of the relatively homogeneous meadow.

The analysis of single random pixels in relation to the surface of the large pixel (30-m) revealed a very high level of agreement in the case of EVI. This is associated with the low spatial variability of the indicator, whose algorithmic design allows enhancement of the vegetation data. This indicates greater possibilities of using low-resolution data for precise spatial analysis. There were no similar correlations for NDVI and GLI, where the statistical parameters were lower by an order of magnitude.

It was found that, regardless of the method used for upscaling the high-resolution data, the results were similar. Only the arithmetic mean differed from

that calculated using the other resampling techniques; in the case of EVI, all techniques yielded similar effects, which should be associated with the characteristics of this indicator mentioned above.

CONCLUSIONS

The spatial variability of the indices is very strongly correlated with the type of land use.

The use of high-resolution data is not advisable in the context of the spatial variability of seasonal vegetation indices in the case of a terrain with homogeneous land cover. The temporal course of structurally simplified indices is less homogeneous than that of indicators with greater complexity consisting of a greater number of modifying factors. Based on the investigations presented in this article, it can be concluded that EVI is the best-suited indicator for upscaling.

Regardless of the method for data averaging, the convergence of information between randomly selected high-resolution pixels and a field with a lower resolution yields good results in the case of EVI.

The analysed GLI indicator exhibits the lowest potential for use in terms of spatial resolution for analyses of areas characterised by homogeneous land use.

FUNDING

The research was financed by the National Science Center (NCN, Poland) grant No. 2016/21/D/ST10/01947.

REFERENCES

- [1] Bannari, A., Morin, D., Bonn, F., Huete, A., 1995. *A review of vegetation indices*. Remote Sensing Reviews, 13: 95–120. DOI: 10.1080/02757259509532298.
- [2] Barrero, O., Perdomo, S.A., 2018. *RGB and multispectral UAV image fusion for Gramineae weed detection in rice fields*. Precision Agriculture, 19: 809–822.
- [3] Caras, T., Hedley, J., Karnielia, A., 2017. *Implications of sensor design for coral reef detection: Upscaling ground hyperspectral imagery in spatial and spectral scales*. International Journal of Applied Earth Observation and Geoinformation, 63: 68–77.
- [4] Fawcett, D., Panigada, C., Tagliabue, G., Boschetti, M., Celesti, M., Evdokimov, A., Biriukova, K., Colombo, R., Miglietta, F., Rascher, U., Anderson, K., 2020. *Multi-scale evaluation of drone-based multispectral surface reflectance and vegetation indices in operational conditions*. Remote Sensing, 12: 514.
- [5] Fraga, H., Amraoui, M., Malheiro, A.C., Moutinho-Pereira, J., Eiras-Dias, J., Silvestre, J., Santos, J.A., 2014. *Examining the relationship between the Enhanced Vegetation Index and grapevine phenology*. European Journal of Remote Sensing, 47: 753–771. DOI: 10.5721/EuJRS20144743.

- [6] Gao, L., Wang, X., Johnson, B. A., Tian, Q., Wang, Y., Verrelst, J., Mu, X., Gu, X., 2020. *Remote sensing algorithms for estimation of fractional vegetation cover using pure vegetation index values: A review*. ISPRS Journal of Photogrammetry and Remote Sensing, 159: 364–377. DOI 10.1016/j.isprsjprs.2019.11.018.
- [7] Hall, C.A., Meyer, W.W., 1976. *Optimal error bounds for cubic spline interpolation*. Journal of Approximation Theory, 16: 105–122. DOI: 10.1016/0021-9045(76)90040-X.
- [8] Heiskanen, J., Liu, J., Valbuena, R., Aynekulu, E., Packalen, P., Pellikka, P., 2017. *Remote sensing approach for spatial planning of land management interventions in West African savannas*. Journal of Arid Environments, 140: 29–41.
- [9] Huete, A.R., 1988. *A soil-adjusted vegetation index (SAVI)*. Remote Sensing of Environment, 25: 295–309. DOI: 10.1016/0034-4257(88)90106-X.
- [10] Huete, A., Didan, K., Miura, T., Rodriguez, E.P., Gao, X., Ferreira, L.G., 2002. *Overview of the radiometric and biophysical performance of the MODIS vegetation indices*. Remote Sensing of Environment, 83: 195–213. DOI: 10.1016/S0034-4257(02)00096-2.
- [11] Hwang, T., Song, C., Bolstad, P.V., Band, L.E., 2011. *Downscaling real-time vegetation dynamics by fusing multi-temporal MODIS and Landsat NDVI in topographically complex terrain*. Remote Sensing of Environment, 115: 2499–2512.
- [12] Karkauskaite, P., Tagesson, T., Fensholt, R., 2017. *Evaluation of the plant phenology index (PPI), NDVI and EVI for start-of-season trend analysis of the Northern Hemisphere boreal zone*. Remote Sensing, 9: 485. DOI:10.3390/rs9050485.
- [13] Kim, D., Silva, R.R., Kim, J., Kim, Y., Kim, H., Chung, J.S., 2020. *Comparison of various kinds of vegetative indices for chlorophyll contents using low-resolution camera*. Journal of Crop Science and Biotechnology, 23: 73–79. DOI: 10.1007/s12892-019-0347-0.
- [14] Li, F., Chen, W., Zeng, Y., Zhao, Q., Wu, B., 2014. *Improving estimates of grassland fractional vegetation cover based on a pixel dichotomy model: A case study in Inner Mongolia, China*. Remote Sensing, 6: 4705–4722. DOI: 10.3390/rs6064705.
- [15] Liu, K., Wang, S., Li, X., Li, Y., Zhang, B., Zhai, R., 2020. *The assessment of different vegetation indices for spatial disaggregating of thermal imagery over the humid agricultural region*. International Journal of Remote Sensing, 41: 1907–1926. DOI: 10.1080/01431161.2019.1677969
- [16] Liu, W., Zenga, Y., Lic, S., Huang, W., 2020. *Spectral unmixing based spatiotemporal downscaling fusion approach*. International Journal of Applied Earth Observation and Geoinformation, 88: 102054.
- [17] Lyons, M.B., Keith, D.A., Phinn, S.R., Mason, T.J., Elith, J., 2018. *A comparison of resampling methods for remote sensing classification and accuracy assessment*. Remote Sensing of Environment, 208: 145–153.
- [18] Mancino, G., Ferrara, A., Padula, A., Nolè, A., 2020. *Cross-comparison between Landsat 8 (OLI) and Landsat 7 (ETM+) derived vegetation indices in a Mediterranean environment*. Remote Sensing, 12: 291.
- [19] Marín, J., Yousfi, S., Mauri, P.V., Parra, L., Lloret, J., Masaguer, A., 2020. *RGB vegetation indices, NDVI, and biomass as indicators to evaluate C3 and C4 turfgrass under different water conditions*. Sustainability, 12: 2160.
- [20] Melesse, A.M., Weng, Q., Thenkabail, P.S., Senay, G.B., 2007. *Remote sensing sensors and applications in environmental resources mapping and modelling*. Sensors, 7: 3209–3241. DOI: 10.3390/s7123209.
- [21] Moreira, A., Bremm, C., Fontana, D.C., Kuplich, T.M., 2017. *Seasonal dynamics of vegetation indices as a criterion for grouping grassland*. Scientia Agricola, 76: 24–32.
- [22] Ovakoglou, G., Alexandridis, T.K., Clevers, J., Gitas, I., 2020. *Downscaling of MODIS leaf area index using Landsat vegetation index*. Geocarto International. DOI: 10.1080/10106049.2020.1750062.

- [23] Palanisamy, S., Rathika, S., Thanakkan, R., Ponnusamy, J., 2019. *Applications of remote sensing in agriculture – a review*. International Journal of Current Microbiology and Applied Sciences, 8: 2270–2283. DOI: 10.20546/ijemas.2019.801.238.
- [24] Planet Team, 2020. *Planet Application Program Interface: In Space for Life on Earth*. Available online: <https://api.planet.com> (access: 03.01.2020).
- [25] Press, W.H., Teukolsky, S.A., Vetterling, W.T., Flannery, B.P., 1992. *Numerical Recipes in C: The Art of Scientific Computing*. Cambridge University Press, New York, pp. 123–128.
- [26] Prey, L., Schmidhalter, U., 2019. *Simulation of satellite reflectance data using high-frequency ground based hyperspectral canopy measurements for in-season estimation of grain yield and grain nitrogen status in winter wheat*. ISPRS Journal of Photogrammetry and Remote Sensing, 149: 176–187.
- [27] Purevdorj, T.S., Tateishi, R., Ishiyama, T., Honda, Y., 1998. *Relationships between percent vegetation cover and vegetation indices*. International Journal of Remote Sensing, 19: 3519–3535. DOI: 10.1080/014311698213795.
- [28] Sharma, K.V., Khandelwal, S., Kaul, N., 2020. Downscaling of coarse resolution land surface temperature through vegetation indices based regression models. In J. Ghosh, I. da Silva (eds.) *Applications of Geomatics in Civil Engineering. Lecture Notes in Civil Engineering*. Springer, Singapore.
- [29] Shirsath, P.B., Sehgal, V.K., Aggarwal, P.K., 2020. *Downscaling regional crop yields to local scale using remote sensing*. Agriculture, 10: 58. DOI: 10.3390/agriculture10030058.
- [30] Sousa, V., Salami, G., Silva, M., Monteiro, J., Alba, E., 2019. *Methodological evaluation of vegetation indexes in land use and land cover (LULC) classification*. Geology, Ecology, and Landscapes. DOI: 10.1080/24749508.2019.160840.
- [31] Tao, J., Dong, J., Zhang, Y., Yu, X., Zhang, G., Cong, N., Zhu, J., Zhang, X., 2020. *Elevation-dependent effects of growing season length on carbon sequestration in Xizang Plateau grassland*. Ecological Indicators, 110: 105880.
- [32] Teillet, P.M., Staenz, K., William, D.J., 1997. *Effects of spectral, spatial, and radiometric characteristics on remote sensing vegetation indices of forested regions*. Remote Sensing of Environment, 61: 139–149.
- [33] Thenkabail, P.S., Lyon, J.G., Huete, A., 2019. Fifty years of advances in hyperspectral remote sensing of agriculture and vegetation – summary, insights, and highlights of volume IV advanced applications in remote sensing of agricultural crops and natural vegetation. In P.S. Thenkabail, J.G. Lyon, A. Huete (eds.), *Advanced Applications in Remote Sensing of Agricultural Crops and Natural Vegetation*, CRC Press.
- [34] Xue, J., Su, B., 2017. *Significant remote sensing vegetation indices: A review of developments and applications*. Journal of Sensors, 1: 1–17. DOI: 10.1155/2017/1353691.